Locking and Noise Properties of Multisection Semiconductor Lasers With Optical Injection. Application to Fabry–Pérot and DFB Cavities

Fabien Kéfélian and Philippe Gallion, *Senior Member, IEEE*

***Abstract*—An analytical theory is presented for the study of injection locking in multisection semiconductor lasers. The Helmoltz equation for the electric field is solved using the Green's function method and the injected fields are included via the boundary conditions. Two cases are distinguished, injection through the front facet of the laser and injection through the rear facet. In both cases, an equation of evolution for the envelope of the electric field is established, taking into account the longitudinal distribution of the carrier and photon densities and the nonlinear gain. The expressions of the intensity, phase and carrier density noise spectra are derived using a matrix formulation. Comparison to classical equations used for Fabry–Pérot lasers is discussed. The locking properties of a distributed feedback laser with an antireflection coated front facet are studied in detail. Results demonstrate the strong sensitivity of the locking properties on the phase grating and rear facet reflectivity.**

***Index Terms*—Distributed-feedback lasers, injection-locked oscillators, optical noise, semiconductor lasers.**

I. Introduction

OPTICAL injection locking is a powerful technique to improve the performance of diode lasers and realize new techniques in telecommunications [1]–[5]. It is also a very interesting phenomenon in terms of physics and nonlinear dynamics [6]–[9] and can be used as a tool for determining fundamental laser parameters [10], [11]. Optical injection locking was first experimentally demonstrated more than forty years ago in gas lasers [12] and its study in semiconductor lasers started in the early 1980s [13], [14] (see [15] for an extended bibliography on the history of optical injection). Contrary to conventional lasers, semiconductor lasers allow a significant fraction of the light to escape and are consequently more sensitive to external perturbations. Moreover, the important dependence of the refractive index on the carrier density in semiconductor lasers has been shown to significantly affect the injection locking properties [16]. The first works on injection locking in semiconductor lasers were mainly dedicated to the study of the range of locking, the stability [17], [18], and the noise properties [19]–[21]. Their results have demonstrated the interest of this technique for frequency stabilization and linewidth narrowing. The analysis of the modulation properties of a locked diode laser has shown the possibility to reduce the relaxation oscillations [22], [23], extend the modulation bandwidth, generate phase modulation and to reduce the chirp [21], [24], [25]. The influence of the gain compression has been also investigated [26] and has been shown to be a factor contributing to stabilization of the locking [27].

Optical injection in semiconductor lasers has been mainly studied using simple rate equations for the outgoing electric field and the carrier density. Some authors have derived these rate equations from the full wave-equation [28], [29], or the round-trip time travelling-wave amplifier model [15], but many works have used a modified version of the rate equation for isolated diode laser by phenomenologically introducing the external field with a coupling factor or feed-in rate. Consequently, the expression of the feed-in rate has sometimes not been set clearly or justified correctly. Moreover, for lasers exhibiting spatial hole burning or containing Bragg gratings, such as distributed feedback (DFB) or distributed Bragg reflector (DBR) lasers, rate equations cannot be derived without first using a full longitudinal treatment. DFB lasers with external feedback have been the subject of several theoretical studies [30], [31], but few results have been published concerning injection locking in DFB lasers. Experimental studies [32]–[34] have for example demonstrated that, contrary to a Fabry–Pérot laser, a DFB laser exhibits a symmetric locking range for weak injection, due to the possibility of having a stable oscillation in a mode with higher threshold gain than the free mode. However, an investigation of the locking range as a function of the DFB laser fundamental parameters is still missing.

Different mathematical tools can be used for the full longitudinal treatment of a multisection laser [35]–[40]. Among them, the Green's function method is well appropriate to derive analytical expressions. The Green's function method was introduced by Henry [41] to analyze the spontaneous emission of semiconductor amplifiers and multisection lasers. This work triggered numerous successful studies concerning the dynamics and noise properties of DFB and more generally of multisection lasers [42]–[46]. Tromborg *et al.* used this method to study the effect of spatial hole burning, nonuniform current injection and nonlinear gain on the linewidth of DFB lasers [47], as well as analyzing the stability and the noise and modulation properties [48]–[50]. The coherence collapse conditions were also derived using the same formalism [51]. The influence of the structure of multisection lasers on the phase-amplitude coupling factor and the spon-

Manuscript received April 26, 2007; revised October 22, 2007.

F. Kéfélian was with the Département Communications et Électronique, École Nationale Supérieure des Télécommunications, in association with the Centre National de la Recherche Scientifique, Paris 75634, France. He is now with the Laboratoire de Physique des Lasers, Université Paris-XIII, Villetaneuse 93430, France.

P. Gallion is with the Département Communications et Électronique, École Nationale Supérieure des Télécommunications, in association with the Centre National de la Recherche Scientifique, Paris 75634, France.

Digital Object Identifier 10.1109/JQE.2008.917239

taneous emission rate have been studied with Green's function by Duan *et al.* [52]. An effective phase-amplitude coupling parameter has been defined and including the nonlinear gain new explanations to the rebroadening of the spectrum at high power has been given. More recently, Green's function has been used for new studies of the external optical feedback, concerning the threshold of the coherence collapse [53] and the spectrum of external cavity lasers [54].

In this paper, we present a theoretical study of the injection locking in a multisection laser. This work extends a previous work of Tromborg *et al.* [31] which used the concept of effective coefficients of reflection and transmission. Two questions are at the source of our investigation. For DFB lasers, which "round-trip time" (or which Q-factor) can be used for the expression of the feed-in rate? For symmetric lasers, is there a difference between an injection through the facet from which the emission is observed (front facet), and an injection through the rear facet)? The purpose of the paper is to obtain a general equation of motion for the electric field envelope in both cases of injection through the front and rear facet, and to hereby derive the noise properties of the injection-locked laser.

The paper is organized as follows. In Section II, starting from the equation of propagation and using the Green's function method, we derive an expression for the Fourier transform of the electric field at the output of the laser as a function of the external injected fields to both facets and a Langevin force representing spontaneous emission. The characteristics of the laser are taken into account using effective reflection and transmission coefficients. In Sections III and IV, the equation of motion of the temporal complex envelope of the electric field is calculated, using a Taylor expansion of the effective coefficients of the cavity, for respectively backward and forward injection. For each direction, the rate equations are linearized to give the locking relation and to determine the power spectral densities of the noises in matrix form. In Section V we apply our results, concerning the feed-in rate value, to the Fabry–Pérot cavity and discuss the comparison to the classical expression of Lang. After, the parameter of injection for a DFB laser with an output facet antireflection coated are numerically studied. Finally, the conclusions are summarized in Section VI.

II. Electric Field in Multisection Laser With External Injection

We consider the general configuration of Fig. 1. The section between $z = 0$ and $z = l$ represents the laser (Fabry-Pérot, DFB or multisections). The internal electric field $\vec{E}$ is decomposed into right and left traveling fields $\vec{E}^+$ and $\vec{E}^-$. At each interface we define a reflection and two transmission coefficients: at $z = 0$, r_1, t_{12} (into the laser) and t_{21} (out of the laser); at $z = l$, r_2, t_{23} (out of the laser) and t_{32} (into the laser). The laser can generally emit light via both facets, but all along the paper we consider that only the field $\vec{E}^+_{\rm out}$ emitted through the right facet ($z = l$) is observed and studied. The right facet is consequently called the front facet, and the left facet is called the rear facet. We assume that an electric field $\vec{E}^-_{\rm injR}$ can be injected through the front facet, using a coupler or a circulator, or that an electric

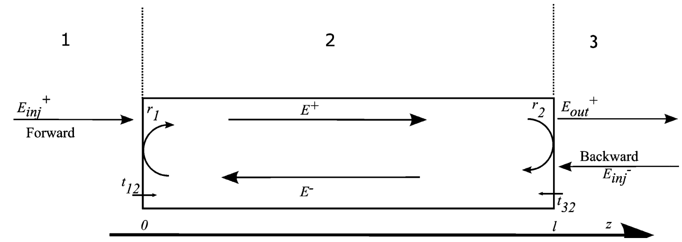

Fig. 1. Laser submitted to the injection by both facets.

field, $\vec{E}^+_{\rm injL}$, can be injected through the rear facet. The starting point is the equation of propagation of the electric field established using the Maxwell's equations in a macroscopic medium

$$\vec{\nabla}^2\vec{E}(\vec{r},t) - \mu_0\sigma\frac{\partial\vec{E}}{\partial t}(\vec{r},t) - \frac{1}{c^2}\frac{\partial^2\vec{E}}{\partial t^2}(\vec{r},t) = \mu_0\frac{\partial^2\vec{P}}{\partial t^2}(\vec{r},t) \quad (1)$$

with $\vec{r} = (x, y, z)$ the position, $\vec{P}$ the electric polarization, μ_0 and ϵ_0 the magnetic permeability and electric permittivity of the vacuum, c the light velocity, and σ the conductivity. $\vec{P}$ can been expressed as a function of the electric field introducing the susceptibility χ. The spontaneous electric polarization, due to quantification of the field, is included using a random function, $\vec{P}_s$

$$\vec{P}(\vec{r},t) = \epsilon_0\chi(\vec{r},t) * \vec{E}(\vec{r},t) + \vec{P}_s(\vec{r},t). \quad (2)$$

Susceptibility and conductivity can be taken into account together through the relative dielectric constant ϵ_r

$$\epsilon_r(\vec{r},\omega) = 1 + \chi(\vec{r},\omega) - j\frac{\sigma(\vec{r},\omega)}{\epsilon_0\omega} \quad (3)$$

with ω the Fourier angular frequency.

The Fourier transform of the electric field is a solution of the Helmoltz equation

$$\vec{\nabla}^2\vec{E}(\vec{r},\omega) + \frac{\omega^2}{c^2}\epsilon_r(\vec{r},\omega)\vec{E}(\vec{r},\omega) = \vec{F}(\vec{r},\omega) \quad (4)$$

with $\vec{F}(\vec{r},\omega) = -\omega^2\mu_0\vec{P}_s(\vec{r},\omega)$. $\vec{F}$ is a Langevin force whose correlation coefficient is given by the theorem of fluctuation dissipation [55]

$$\langle\vec{F}(\vec{r'},\omega)\vec{F}^*(\vec{r},\omega')\rangle = 2D_{\vec{F}\vec{F}^*}\delta(\vec{r}-\vec{r'},\omega-\omega') \quad (5)$$

$$D_{\vec{F}\vec{F}^*}(\vec{r},\omega) = \frac{2\pi\omega^3\hbar}{c^3\epsilon_0}n_m(\vec{r})g_m(\vec{r})n_{\rm sp} \quad (6)$$

$$n_{\rm sp} = \frac{1}{1 - e^{\left(\frac{\hbar\omega - E_{cv}}{k_B T}\right)}} \quad (7)$$

with T the temperature, k_B the Boltzmann constant, h the Planck constant, $\hbar = h/2\pi$, E_{cv} the energy difference between the quasi-Fermi levels, $n_m = \sqrt{\Re e\{\epsilon_r\}}$ the material refractive index, $g_m = (\omega/cn_m)\Im m\{\chi\}$ the material gain, and $n_{\rm sp}$ the inversion factor.

We assume that, in each section i of the laser, the electric field oscillates in the fundamental transverse mode $\Phi_i(x, y)$ polarized along $\vec{u}$ with the complex constant of propagation $k_i(z,\omega)$ satisfying [56]

$$\left[\frac{\partial^2}{\partial x^2}+\frac{\partial^2}{\partial y^2}+\frac{\omega^2}{c^2}\epsilon_r(x,y,z,\omega)\right]\Phi_i(x,y)=k_i^2(z,\omega)\Phi_i(x,y). \tag{8}$$

Consequently $\vec{E}(\vec{r},\omega)$ can be written as $E(z,\omega)\Phi_i(x,y)\vec{u}$ with $E(z,\omega)$ satisfying

$$\left[\frac{\partial^2}{\partial z^2}+k^2(z,\omega)\right]E(z,\omega)=f(z,\omega) \tag{9}$$

where

$$f(z,\omega)=\frac{\int\int \vec{F}(x,y,z,\omega)\Phi(x,y)\vec{u}\,dx\,dy}{\int\int \Phi(x,y)\Phi(x,y)\,dx\,dy} \tag{10}$$

represents the spontaneous emission in the transverse mode.

Solving the inhomogeneous differential equation (9) using the Green's function method (Appendix A), the Fourier transform of the forward traveling component of the electric field at the front facet of the laser can be expressed as a function of the injected fields and a Langevin force

$$E^+(l^-,\omega)=\frac{t_Lt_{12}E^+_{\mathrm{injL}}(0^-,\omega)+r_Lt_{32}E^-_{\mathrm{inj}R}(l^+,\omega)+F_L}{[1-r_2r_L]} \tag{11}$$

where r_L and t_L are the equivalent reflection and transmission coefficients of the active region between $z=0^-$ and $z=l^-$ for a backward traveling wave and F_L is a Langevin force representing the total spontaneous emission at the output of the laser. Expressions of r_L, t_L and F_L are derived in Appendix A.

III. Dynamic Equations and Noise Properties of Laser Diode With Backward Injection

We consider in this section the injection of a backward traveling wave $\vec{E}^-_{\mathrm{inj}R}$ through the front facet, i.e., backward injection.

A. Expansion of the Electric Field Equation

For injection through the front facet (11) becomes

$$\frac{E^+(l^-,\omega)}{r_L}=r_2E^+(l^-,\omega)+t_{32}E^-_{\mathrm{inj}R}(l^+,\omega)+\frac{F_L(\omega)}{r_L} \tag{12}$$

r_L depends on ω, but also on the carrier and photon densities $\mathcal{N}(z)$ and $\mathcal{P}(z)$, via ϵ_r. Since $\mathcal{N}$ and $\mathcal{P}$ depend on z, r_L is a functional, i.e., a function of functions.

$\mathcal{P}(z)$ is the transversely average photon density in the active layer (AL)

$$\mathcal{P}(z)=\frac{2\epsilon_0\mathrm{nn_{g}}_{ca}(z)\,n_{gm}\Gamma}{\hbar\omega_0A_{\mathrm{act}}}|E(z)|^2 \tag{13}$$

where $\mathrm{nn_{g}}_{ca}(z)$ is the value of the product of the material refractive index and the group refractive index $n_{gm}=n_m+\omega\partial n_m/\partial\omega$ transversally average on the AL

$$\mathrm{nn_{g}}_{ca}(z)=\frac{1}{A_{\mathrm{act}}}\int\int_{AL}n_m(\vec{r})n_{gm}(\vec{r})|\Phi(x,y)|^2\,dx\,dy. \tag{14}$$

Γ is the confinement factor of the transverse mode in the AL and A_{act} the transverse area of the AL [56].

Without injection, when spontaneous emission is neglected, the static solution $(\omega_s,\mathcal{N}_s(z),\mathcal{P}_s(z))$ fulfills the condition of oscillation

$$r_2r_L(\omega_s,\mathcal{N}_s(z),\mathcal{P}_s(z))=1. \tag{15}$$

When the laser is submitted to optical injection, the static parameters of the laser are modified. Once locking is achieved, the central frequency of the slave laser becomes equal to the central frequency of the master laser ω_i. Assuming that the function $1/r_L$ is slowly varying in a region around $(\omega_s,\mathcal{N}_s,\mathcal{P}_s)$, and that the detuned state with deviation $\Delta\mathcal{N}$ and $\Delta\mathcal{P}$ is included in this region, the value of $1/r_L$ can be determined using a Taylor expansion

$$\begin{aligned}\frac{1}{r_L(\omega,\mathcal{N},\mathcal{P})}\approx{}&\frac{1}{r_{Ls}}+\left[\frac{\partial\frac{1}{r_L}}{\partial\omega}\right]_s(\omega-\omega_s)\\&+\int_0^l\left[\frac{\delta\frac{1}{r_L}}{\delta k}(z)\frac{\partial k}{\partial\mathcal{N}}\right]_s(\Delta\mathcal{N}(z))\,dz\\&+\int_0^l\left[\frac{\delta\frac{1}{r_L}}{\delta k}(z)\frac{\partial k}{\partial\mathcal{P}}\right]_s(\Delta\mathcal{P}(z))\,dz.\end{aligned} \tag{16}$$

$\delta 1/r_L$ is the functional derivative of $1/r_L$ introduced by Tromborg *et al.* in [47]

$$\delta\frac{1}{r_L}=\int_0^l\frac{\delta\frac{1}{r_L}}{\delta k}(z)\delta k(z)\,dz \tag{17}$$

where $\delta(1/r_L)/\delta k$ represents the infinitesimal variation of $1/r_L$ due to an infinitesimal variation δk of the function k.

B. Temporal Envelope of the Electric Field

The complex envelope around ω_i of the forward traveling component of the intracavity electric field at the front facet is defined by

$$A^+(t)=\frac{1}{2\pi}\int_0^\infty E^+(l^-,\omega)e^{j(\omega-\omega_i)t}d\omega. \tag{18}$$

The envelope of the injected field $A^i(t)$ is defined similarly in l^+.

Using the expansion of $1/r_L$ in the equation (12), the equation of motion of A^+ can be obtain by inverse Fourier transform

$$\begin{aligned}\frac{dA^+}{dt}(t)={}&-j(\omega_s-\omega_i)A^+(t)+A^+(t)\langle C_{\mathcal{N}}\,|\,\Delta\mathcal{N}(t)\rangle\\&+A^+(t)+\langle C_{\mathcal{P}}\,|\,\Delta\mathcal{P}(t)\rangle+f_Rt_{32}A^i(t)+F_A(t)\end{aligned} \tag{19}$$

with

$$f_R = r_{Ls} f_D = j \left(\frac{\partial \frac{1}{r_L}}{\partial \omega} \right)_s^{-1} \tag{20}$$

$$C_{\mathcal{N}}(z) = - \left[\frac{\delta \frac{1}{r_L}}{\delta k}(z) \frac{\partial k}{\partial \mathcal{N}} \right]_s f_R \tag{21}$$

$$C_{\mathcal{P}}(z) = - \left[\frac{\delta \frac{1}{r_L}}{\delta k}(z) \frac{\partial k}{\partial \mathcal{P}} \right]_s f_R. \tag{22}$$

We use here a notation similar to the notation of Dirac in quantum mechanics

$$\langle f \,|\, g \rangle = \int_0^l f(z')g(z')dz'. \tag{23}$$

The derivatives of k are given by

$$\frac{\partial k}{\partial \omega} = \frac{1}{v_g} + \frac{j}{2}\frac{\partial g}{\partial \omega} \tag{24}$$

$$\frac{\partial k}{\partial \mathcal{N}} = j \frac{1 + j\alpha_H}{2} \frac{\partial g}{\partial \mathcal{N}} \tag{25}$$

with $\alpha_H = -2k(\partial n/\partial \mathcal{N}/\partial g/\partial \mathcal{N})$ the Henry factor, g the modal gain, n the modal refractive index and v_g the group velocity.

The first term on the right-hand side of (19) represents the rotation of A^+ due to the detuning, the second and third ones represent the in phase and in quadrature contributions due to the modification of the gain and index induced by the carrier and photon density modifications. The functions $C_{\mathcal{N}}$ and $C_{\mathcal{P}}$ determine the variation of the global gain and index of the cavity due to the local variation in z of the carrier and photon densities. They take into account longitudinal spatial hole burning [57] and spectral-hole burning [58]. The fourth term represents the contribution of the injected field. F_A is the Langevin force representing the contribution of the spontaneous emission to the envelope evolution

$$F_A(t) = \frac{f_D}{2\pi} \int_0^\infty F_L(\omega) e^{j(\omega - \omega_i)t}\, d\omega. \tag{26}$$

The autocorrelation of F_A is derived from (6), (10), (26), and (98) (Appendix A)

$$\langle F_A(t) F_A^*(t') \rangle = \frac{R_{\rm sp}}{\sigma_p^2} \delta(t - t') \tag{27}$$

with

$$R_{\rm sp} = \frac{4\omega_0^3 \hbar \langle \mathrm{nn_g} \,|\, |Z_L|^2 \rangle |f_D|^2 \langle \mathrm{ng} n_{\rm sp} \,|\, |Z_L|^2 \rangle |Z_1^+(0)|^2}{c^3 \left| \int\int \Phi(x,y)\Phi(x,y)\, dx\, dy \right|^2 |Z_2^-(l)|^2} \tag{28}$$

where the Z functions are defined in Appendix A. $R_{\rm sp}$ is the average rate of spontaneous emission into the mode, taking into account the effect of the transverse mode [59] and the longitudinal mode [41], [47], [31] on the standard relation of Einstein $R_{\rm sp} = v_g g n_{\rm sp}$. σ_p is a constant such that $p = \sigma_p^2 |A|^2$ is the total number of photons in the laser cavity

$$\sigma_p^2 = 2 \frac{\epsilon_0}{\hbar \omega_s} \int \mathrm{nn_g}(z) |Z_L(z)|^2 dz \tag{29}$$

with

$$\mathrm{nn_g}(z) = \int\int n(\vec{r}) n_g(\vec{r}) |\Phi(x,y)|^2\, dx\, dy \tag{30}$$

$$\mathrm{ng}(z) = \int\int n_m(\vec{r}) g_m(\vec{r}) |\Phi(x,y)|^2\, dx\, dy. \tag{31}$$

C. Optical Phase and Power Equations

The mean optical power I emerging from the front facet of the laser is given by

$$I(t) = T_2 \sigma_I^2 |A^+(t)|^2 \tag{32}$$

where $\sigma_I^2 = 2\epsilon_0 c n_g(l^-)$, n_g is the modal group refractive index and $T_2 = 1 - |r_2|^2$. The incident optical power $I_{\rm in}(t)$ is similarly given by

$$I_{\rm in}(t) = \frac{\sigma_I^2}{n_g(l^-)} |A_{\rm in}(t)|^2. \tag{33}$$

The rate equations for the output power $I(t)$ and the phase of A^+, $\phi(t)$, are determined by multiplication of (19) by $4A^{+*}\epsilon_0 c n_g(l^-) T_2$ and separation into real and imaginary parts

$$\begin{aligned} \frac{dI}{dt}(t) = {} & 2I(t)\langle \Re e\{C_{\mathcal{N}}\} \,|\, \Delta\mathcal{N}(t) \rangle + 2I(t) \langle \Re e\{C_{\mathcal{P}}\} \,|\, \Delta\mathcal{P}(t) \rangle \\ & + 2T_2 \sqrt{I(t) I_{\rm in}(t)} |f_R| \cos(\theta(t) + \psi_R) + F_I(t) \end{aligned} \tag{34}$$

$$\begin{aligned} \frac{d\phi}{dt}(t) = {} & (\omega_s - \omega_i) + \langle \Im m\{C_{\mathcal{N}}\} \,|\, \Delta\mathcal{N}(t) \rangle + \langle \Im m\{C_{\mathcal{P}}\} \,|\, \Delta\mathcal{P}(t) \rangle \\ & + T_2 \sqrt{\frac{I_{\rm in}(t)}{I(t)}} |f_R| \sin(\theta(t) + \psi_R) + F_\phi(t) \end{aligned} \tag{35}$$

where $\theta(t) = \phi_{\rm in}(t) - \phi(t)$, $\phi_{\rm in}$ is the phase of A^i and $\psi_R = \arg\{f_R\}$.

The carrier density is governed by the rate equation

$$\begin{aligned} \frac{d\mathcal{N}(z,t)}{dt} = {} & J(z,t) - \mathrm{R}(\mathcal{N}(z,t)) \\ & - v_g g(\mathcal{N}(z,t), \mathcal{P}(z,t)) \mathcal{P}(z,t) + F_{\mathcal{N}}(z,t) \end{aligned} \tag{36}$$

where J is the density of injected carriers, R is the function describing the spontaneous recombination of the carriers and $F_{\mathcal{N}}(z,t)$ is the Langevin force associated to the fluctuation of carriers due to the interaction between the field and the spontaneous electric polarization [60].

The nonzero Langevin forces diffusion coefficients are [61]

$$2D_{II} = 2R_{\rm sp} I_0 T_2 \left(\frac{\sigma_I}{\sigma_p} \right)^2 \tag{37}$$

$$2D_{\phi\phi} = \frac{R_{\rm sp}}{2p_0} \tag{38}$$

$$2D_{\mathcal{N}\mathcal{N}}(z) = 2 \frac{[v_g g_0(z) n_{\rm sp} \mathcal{P}_0(z) + \mathrm{R}(\mathcal{N}(z))]}{A_{\rm act}} \tag{39}$$

$$2D_{I\mathcal{N}}(z) = -2v_g g_0(z) n_{\mathrm{sp}} \mathcal{P}_0(z) T_2 \left(\frac{\sigma_I}{\sigma_p}\right)^2 \tag{40}$$

D. Calculation of the Locking Range

Locked states $(\theta_0, I_0, \mathcal{N}_0(z), \mathcal{P}_0(z))$ are solutions of (34), (35) and (36) with all noise and derivative terms set to zero. When locking is achieved, the phase difference and angular frequency detuning are related by

$$\omega_i - \omega_s = \eta_b |f_R| \sqrt{1+\alpha_{\mathrm{eff}}^2} \sin(\theta_0 + \psi_R - \tan^{-1}(\alpha_{\mathrm{eff}})) \tag{41}$$

where $\eta_b = \sqrt{(I_{\mathrm{in}0}T_2/I_0/T_2)}$, η_b^2 is the ratio between the optical power injected through the front facet and the forward traveling intracavity optical power at the front facet. It is important to point out here that, for a locked state, it is possible to define a stationary mean value of the difference of the slave and master phases, but not of the individual phases which remain unstationary random functions. A generalized Henry factor has been used

$$\alpha_{\mathrm{eff}} = \frac{\langle \Im m\{C_\mathcal{N}\} \,|\, \Delta\mathcal{N}\rangle + \langle \Im m\{C_\mathcal{P}\} \,|\, \Delta\mathcal{P}\rangle}{\langle \Re e\{C_\mathcal{N}\} \,|\, \Delta\mathcal{N}\rangle + \langle \Re e\{C_\mathcal{P}\} \,|\, \Delta\mathcal{P}\rangle} \tag{42}$$

taking into account the impact of the longitudinal distribution of the carrier and photon densities, and the gain compression. The imaginary part of $C_\mathcal{P}$, corresponding to a modification of the refractive index induced by the photon density modification, is generally negligible. The maximum detuning is

$$\max\{\omega_i - \omega_s\} = \eta_b |f_R| \sqrt{1+\alpha_{\mathrm{eff}}^2}. \tag{43}$$

Since α_{eff} is not a material parameter but rather a structural parameter, it depends in fact on the condition of injection. Consequently, the exact locking range must be calculated self-consistently. Stability of the solutions inside the locking range can be discussed using the Hurwitz criterion on the small signal equations.

E. Determination of the Power Spectral Densities of Noise

The longitudinal mode $Z_L(z)$ depends on ω, $\mathcal{P}$ and $\mathcal{N}$. Consequently $\mathcal{P}(t)$ cannot be directly related to $I(t)$ using the group velocity. The following expression, determined by Tromborg *et al.* [47], is used for $\mathcal{P}(t)$ to take into account these dependences

$$|\delta\mathcal{P}\rangle = (1-\mathfrak{M}_\mathcal{P})^{-1}\left[|\mathcal{P}_0\rangle \frac{\delta I}{I_0} + \frac{|H_I\rangle}{2I_0}\frac{d\delta I}{dt} + |H_\phi\rangle \frac{d\phi}{dt}\right] + \mathfrak{M}|\delta\mathcal{N}\rangle. \tag{44}$$

Expression for the different functions and operators are recalled in Appendix B. The rate equations of (34), (35) and (36) are linearized around the static point $(I_0, I_{\mathrm{in}0}, \theta_0, \mathcal{N}_0(z))$. $(\delta I, \delta I_{\mathrm{in}}, \delta\theta, \delta\mathcal{N}(z))$ is the deviation to the static point induced by noise. Due to the unstationarity of the phase noise, $\delta\phi$ or $\delta\phi_{\mathrm{in}}$ cannot be defined. Using the following vectorial notations [62]:

$$\boldsymbol{X}(\Omega) = \begin{bmatrix} \delta I(\Omega) \\ \phi(\Omega) \\ \delta\mathcal{N}(\Omega, z) \end{bmatrix} \tag{45}$$

$$\boldsymbol{X}_{\mathbf{in}}(\Omega) = \begin{bmatrix} \delta I_{\mathrm{in}}(\Omega) \\ \phi_{\mathrm{in}}(\Omega) \\ \delta\mathcal{N}_{\mathrm{in}}(\Omega, z) \end{bmatrix} \tag{46}$$

$$\boldsymbol{F}(\Omega) = \begin{bmatrix} F_I(\Omega) \\ F_\phi(\Omega) \\ F_\mathcal{N}(\Omega, z) + \delta J(\Omega, z) \end{bmatrix} \tag{47}$$

the expression of the noises can be expressed by

$$\boldsymbol{X}(\Omega) = ([M(\Omega)] + [D])^{-1}([C]\boldsymbol{X}_{\mathrm{in}}(\Omega) + \boldsymbol{F}(\Omega)) \tag{48}$$

Noting

$$k_c = \eta_b\,|f_R|\,\cos(\theta_0 + \psi_R)$$
$$k_s = \eta_b\,|f_R|\,\sin(\theta_0 + \psi_R)$$

the coefficients of the matrix $[M]$, $[D]$, and $[C]$ are given by

$$\begin{aligned}
m_{11} &= -2\langle C_{\mathcal{N}r} \,|\, \Delta\mathcal{N}_0\rangle - 2\langle C_{\mathcal{P}r} \,|\, \Delta\mathcal{P}_0\rangle \\
&\quad - 2\langle C_{\mathcal{P}r}|(1-\mathfrak{M}_\mathcal{P})^{-1}|\mathcal{P}_0\rangle \\
&\quad - j\Omega\langle C_{\mathcal{P}r}|(1-\mathfrak{M}_\mathcal{P})^{-1}|H_I + j\Omega\rangle \\
m_{12} &= -j\Omega 2I_0\langle C_{\mathcal{P}r}|(1-\mathfrak{M}_\mathcal{P})^{-1}|H_\phi\rangle \\
m_{13} &= -2I_0\langle C_{\mathcal{N}r}| - \langle C_{\mathcal{P}r}|\mathfrak{M} \\
m_{21} &= -\frac{1}{I_0}\langle C_{\mathcal{P}i}|(1-\mathfrak{M}_\mathcal{P})^{-1}|\mathcal{P}_0\rangle \\
&\quad - \frac{j\Omega}{2I_0}\langle C_{\mathcal{P}i}|(1-\mathfrak{M}_\mathcal{P})^{-1}|H_I \\
m_{22} &= -j\Omega\langle C_{\mathcal{P}i}|(1-\mathfrak{M}_\mathcal{P})^{-1}|H_\phi + j\Omega\rangle \\
m_{23} &= -\langle C_{\mathcal{N}i}| - \langle C_{\mathcal{P}i}|\mathfrak{M} \\
m_{31} &= \left[v_g \frac{\partial g}{\partial \mathcal{P}}\mathcal{P}_0(z) + v_g g_0(z)\right] \\
&\quad \times\, (1-\mathfrak{M}_\mathcal{P})^{-1}\left[\frac{|\mathcal{P}_0\rangle}{I_0} + \frac{j\Omega\,|H_I\rangle}{2I_0}\right] \\
m_{32} &= \left[v_g \frac{\partial g}{\partial \mathcal{P}}\mathcal{P}_0(z) + v_g g_0(z)\right] \\
&\quad \times\, (1-\mathfrak{M}_\mathcal{P})^{-1}\,|\,H_\phi\rangle j\Omega \\
m_{33} &= \frac{\partial \mathrm{R}}{\partial \mathcal{N}} + v_g g_N \mathcal{P}_0(z) \\
&\quad + \left[v_g \frac{\partial g}{\partial \mathcal{P}}\mathcal{P}_0(z) + v_g g_0(z)\right]\mathfrak{M} + j\Omega \\
d_{11} &= -k_c \\
d_{12} &= -2I_0\,k_s \\
d_{21} &= -\frac{k_s}{2I_{\mathrm{in}0}} \\
d_{22} &= -k_c \\
c_{11} &= \frac{I_0}{I_{\mathrm{in}0}}k_c \\
c_{12} &= -2I_0\,k_s \\
c_{21} &= \frac{k_s}{2I_{\mathrm{in}0}} \\
c_{22} &= k_c.
\end{aligned} \tag{49}$$

The power spectral densities can be expressed using an Hermitian product

$$S_{\boldsymbol{X}}(\Omega)\delta(\Omega-\Omega') = \langle X(\Omega)X(\Omega')^\dagger\rangle. \tag{50}$$

The coefficients of $S_{\boldsymbol{X}}$ correspond to the power spectral densities of the intensity, phase and carrier density noises for the diagonal terms and to the respective interspectral power densities for the nondiagonal ones. Using (48)

$$S_{\boldsymbol{X}}(\Omega) = ([M]+[D])^{-1}[C]S_{\boldsymbol{X}_{\text{in}}}(\Omega)[C]^{\dagger}([M]+[D])^{-1\dagger} \\ +([M]+[D])^{-1}S_{\boldsymbol{F}}(\Omega)([M]+[D])^{-1\dagger} \quad (51)$$

with

$$S_{\boldsymbol{F}}(\Omega) = 2\begin{bmatrix} D_{II} & 0 & D_{I\mathcal{N}}(z) \\ 0 & D_{\phi\phi} & 0 \\ D_{I\mathcal{N}}(z) & 0 & D_{\mathcal{N}\mathcal{N}}(z)+S_J(\Omega,z) \end{bmatrix}. \quad (52)$$

The linewidth of the injection-locked spectrum can be determined from the value of $S_\phi(\Omega)/\Omega^2$ in $\Omega = 0$. However, for very small values of k_c, $S_\phi(\Omega)/\Omega^2$ is not constant on a sufficiently wide range of frequencies around zero and consequently the power spectrum of the injection-locked laser can no longer be represented by a Lorentzian lineshape.

F. Comments

The coefficients which depend directly on the injected fields are d_{ij} and c_{ij}. c_{ij} indicates how the noise of the injected field $\boldsymbol{X}_{\text{in}}$ is coupled to the intrinsic sources of noise of the slave laser $\boldsymbol{F}$, resulting in an equivalent internal source of noise $[C]\boldsymbol{X}_{\text{in}}(\Omega)+\boldsymbol{F}(\Omega)$. d_{ij} indicates how the injection modifies the response of the laser to the source of noise, which is represented by the coefficients m_{ij}. It is interesting to note that the coefficient d_{ij} and c_{ij} are independent on the structure, they are identical to the Fabry–Pérot case [63]. Inversely, coefficients m_{ij}, which, without injection, determine the noise properties of the laser, depend on the structure of the laser. The terms involving a longitudinal integration take into account the effect of the spatial hole burning and nonuniform current injection. The gain compression effect appears through $C_{\mathcal{P}r}$ and $\partial g/\partial\mathcal{P}$. The use of the expansion of the carrier density noise (44), involved new transfer of noise through the modification of the longitudinal mode represented by the operator $\mathfrak{M}_{\mathcal{P}}$ and $\mathfrak{M}$ and the functions $H(z)$ and $H_I(z)$. This effect leads to an additional coupling between the rate equations of intensity, phase and carrier density which appears specially in the factor m_{12} and m_{32}, which would be null otherwise. Thus, factor m_{12} corresponds to a contribution of the frequency noise to the intensity noise. Such a contribution is generally induced only by injection locking through the factor d_{12} but is here also self-induced. It is due to the fact that the frequency noise induces a noise on the longitudinal distribution of the photon density and consequently a noise on the output power through the gain compression. Factor m_{32} represents a contribution of the frequency noise on the carrier density noise, the frequency noise induces a noise on the longitudinal distribution of the photon density and consequently a noise on the carrier density through the photon-carrier coupling of the gain. Moreover the influence of those two parameters increase with the frequency Ω and consequently can become important for the calculation of the phase noise at frequency offset above 1 GHz. Finally, the gain curve influence is also present through the factor $H(z)$ which is important for emission far from the maximum of the gain curve.

IV. Dynamic Equations and Noise Properties of Laser Diode With Forward Injection

We consider in this section the injection of a forward traveling wave $\vec{E}^{+}_{\text{injL}}$ through the rear facet, i.e., forward injection.

A. Temporal Envelope of the Electric Field

For injection through the rear facet, (11) becomes

$$E^{+}(l^{-},\omega) = r_L r_2 E^{+}(l^{-},\omega) + t_L t_{12} E^{+}_{\text{injL}}(0^{-},\omega) + F_L(\omega) \quad (53)$$

Using the following first-order expansion:

$$\left(\frac{t_L}{r_L}\right)(\omega,\mathcal{N},\mathcal{P}) = \left(\frac{t_L}{r_L}\right)(\omega_s,\mathcal{N}_s,\mathcal{P}_s) + \left(\frac{\partial\frac{t_L}{r_L}}{\partial\omega}\right)_s(\omega-\omega_s) \\ + \int_0^l \left(\frac{\delta\frac{t_L}{r_L}}{\delta k}\right)_s \frac{\partial k}{\partial\mathcal{N}}\Delta\mathcal{N}(z)\,dz \\ + \int_0^l \left(\frac{\delta\frac{t_L}{r_L}}{\delta k}\right)_s \frac{\partial k}{\partial\mathcal{P}}\Delta\mathcal{P}(z)\,dz \quad (54)$$

the equation of motion of the temporal envelope of the forward traveling component of the intracavity electric field at the front facet is established by inverse Fourier transform

$$\frac{dA^{+}}{dt}(t) = -j(\omega_s-\omega_i)A^{+}(t) + A^{+}(t)[\langle C_{\mathcal{N}}|\Delta\mathcal{N}\rangle + \langle C_{\mathcal{P}}|\Delta\mathcal{P}\rangle] \\ + f_T t_{12} A^i(t) + \left[\left\langle C^t_{\mathcal{N}}\right|\Delta\mathcal{N}\rangle + \langle C^t_{\mathcal{P}}\left|\Delta\mathcal{P}\right\rangle\right] t_{12} A^i(t) \\ + \frac{f_T}{f_t}\frac{d\,A^i}{dt}(t) + j\frac{f_T}{f_t}(\omega_i-\omega_s)t_{12}A^i(t) + F_A(t) \quad (55)$$

where

$$f_T = f_D t_{Ls} \\ C^t_{\mathcal{N}} = f_R\left(\frac{\delta\frac{t_L}{r_L}}{\delta k}\frac{\partial k}{\partial\mathcal{N}}\right)_s \\ C^t_{\mathcal{P}} = f_R\left(\frac{\delta\frac{t_L}{r_L}}{\delta k}\frac{\partial k}{\partial\mathcal{P}}\right)_s \\ \frac{r_L}{t_L}f_t = j\left(\frac{\partial\frac{t_L}{r_L}}{\partial\omega}\right)_s^{-1}. \quad (56)$$

The two first terms of the right-hand side of (55) are identical to the case of backward injection, and the four following terms represents the contribution of the injected field. The feed-in rate $f_T t_{12}$ is different from the backward case. Four additional contributions from the injected field appear in the equation. Those contributions come from the effect of the single pass through the cavity by the injected field. The fourth terms represents the modification of the single pass gain and phase rotation due to the deviation of the carrier and photon densities. The fifth term takes into account the delay induced by the single pass trip by introducing a contribution of the derivative of the envelope of the injected field, and the sixth comes from the detuning of the injected frequency from the natural frequency of the cavity.

B. Optical Phase and Power Equations

The equations of motion for the optical phase and the optical power are derived using the same method as for the backward case

$$\begin{aligned}\frac{dI}{dt}(t) &= 2[\langle C_{\mathcal{N}r} \,|\, \Delta\mathcal{N}\rangle + \langle C_{\mathcal{P}r} \,|\, \Delta\mathcal{P}\rangle]I(t)\\ &\quad + 2|f_T|\sqrt{T_1T_2I_{\mathrm{in}}(t)I(t)}\cos(\theta(t)+\psi_T)\\ &\quad + 2\left|\left\langle C_{\mathcal{N}}^t\right|\Delta\mathcal{N}\right\rangle + \left\langle C_{\mathcal{P}}^t\right|\Delta\mathcal{P}\rangle\Big|\sqrt{T_1T_2I_{\mathrm{in}}(t)I(t)}\\ &\quad \times\cos\left(\theta(t)+\arg\left(\left\langle C_{\mathcal{N}}^t\right|\Delta\mathcal{N}\right\rangle + \left\langle C_{\mathcal{P}}^t\right|\Delta\mathcal{P}\rangle\right)\Big)\\ &\quad - 2\left|\frac{f_T}{f_t}\right|(\omega_i-\omega_s)\sqrt{T_1T_2I_{\mathrm{in}}(t)I(t)}\sin(\theta(t)+\psi_t)\\ &\quad + \left|\frac{f_T}{f_t}\right|\frac{dI_{\mathrm{in}}}{dt}(t)\sqrt{\frac{T_1T_2I_{\mathrm{in}}(t)}{I(t)}}\cos(\theta(t)+\psi_t)\\ &\quad - 2\left|\frac{f_T}{f_t}\right|\frac{d\phi_{\mathrm{in}}}{dt}(t)\sqrt{T_1T_2I_{\mathrm{in}}(t)I(t)}\sin(\theta(t)+\psi_t)\\ &\quad + F_I(t) \qquad (57)\\ \frac{d\phi}{dt}(t) &= [\langle C_{\mathcal{N}i} \,|\, \Delta\mathcal{N}\rangle + \langle C_{\mathcal{P}i} \,|\, \Delta\mathcal{P}\rangle] - (\omega_i-\omega_s)\\ &\quad + |f_T|\sqrt{\frac{T_1T_2I_{\mathrm{in}}(t)}{I(t)}}\sin(\theta(t)+\psi_T)\\ &\quad + \left|\left\langle C_{\mathcal{N}}^t\right|\Delta\mathcal{N}\right\rangle + \left\langle C_{\mathcal{P}}^t\right|\Delta\mathcal{P}\rangle\Big|\sqrt{T_1T_2}\sqrt{\frac{I_{\mathrm{in}}(t)}{I(t)}}\\ &\quad \times\sin\left(\theta(t)+\arg\left(\left\langle C_{\mathcal{N}}^t\right|\Delta\mathcal{N}\right\rangle + \left\langle C_{\mathcal{P}}^t\right|\Delta\mathcal{P}\rangle\right)\Big)\\ &\quad + \left|\frac{f_T}{f_t}\right|(\omega_i-\omega_s)\sqrt{\frac{T_1T_2I_{\mathrm{in}}(t)}{I(t)}}\cos(\theta(t)+\psi_t)\\ &\quad + \frac{1}{2}\left|\frac{f_T}{f_t}\right|\frac{dI_{\mathrm{in}}}{dt}(t)\sqrt{\frac{T_1T_2}{I_{\mathrm{in}}(t)I(t)}}\sin(\theta(t)+\psi_t)\\ &\quad + \left|\frac{f_T}{f_t}\right|\frac{d\phi_{\mathrm{in}}}{dt}(t)\sqrt{\frac{T_1T_2I_{\mathrm{in}}(t)}{I(t)}}\cos(\theta(t)+\psi_t)\\ &\quad + F_\phi(t) \qquad (58)\end{aligned}$$

where $\psi_t = \arg\{f_T/F_T\}$. Due to the involvement of the derivative of the temporal envelope of the injected wave, corresponding contributions appear in the equations of motion of the phase and the power.

C. Calculation of the Locking Condition

Locked states are solution of (36), (57) and (58) with all noise and derivative terms set to zero. When locking is achieved, phase difference and angular frequency detuning are related by

$$\begin{aligned}&\omega_i-\omega_s\\ &\quad = \frac{\eta_f\sqrt{1+\alpha_{\mathrm{eff}}^2}}{1-\eta_f\sqrt{1+\alpha_{\mathrm{eff}}^2}\left|\frac{f_T}{f_t}\right|\cos(\theta_0+\psi_t-\tan^{-1}(\alpha_{\mathrm{eff}}))}\\ &\qquad \times\{|f_T|\sin(\theta_0+\psi_T-\tan^{-1}(\alpha_{\mathrm{eff}}))\\ &\qquad + |f_\Delta|\sin(\theta_0+\arg(f_\Delta)-\tan^{-1}(\alpha_{\mathrm{eff}}))\} \qquad (59)\end{aligned}$$

where

$$f_\Delta = \left\langle C_{\mathcal{N}}^t\right|\Delta\mathcal{N}\rangle + \left\langle C_{\mathcal{P}}^t\right|\Delta\mathcal{P}\rangle \qquad (60)$$

and $\eta_f = \sqrt{(I_{\mathrm{in}0}T_1/I_0/T_2)}$, η_f^2 is the ratio between the optical power injected through the rear facet and the forward traveling internal optical power at the front facet. Because f_Δ depends on $\mathcal{P}$ and $\mathcal{N}$, the exact expression of the locking range has to be determined self-consistently.

It could appear surprising to obtain a different expression of the locking range for the backward and the forward injections. In the case of a symmetric laser ($T_1 = T_2$), if we consider the light emitted by the rear facet, the existence of two different expressions seems to allow solutions where for example the forward traveling components of the intracavity field is locked but not the backward one. This is in fact not the case, because the injection modifies the longitudinal distribution of the optical power inside the cavity, and leads to an asymmetry of the emitted power, even for symmetric laser, as was shown in [29] for a Fabry–Pérot cavity. Consequently it is consistent to obtain different expressions for the forward and backward injections.

D. Power Spectral Densities of Noise

Using the notations

$$\begin{aligned}k_c &= \eta_f|f_T|\,\cos(\theta_0+\psi_T) &(61)\\ k_s &= \eta_f|f_T|\,\sin(\theta_0+\psi_T) &(62)\\ \chi_t &= \left|\frac{f_T}{f_t}\right| &(63)\\ \chi_c &= \chi_t\,\cos(\theta_0+\psi_t) &(64)\\ \chi_s &= \chi_t\,\sin(\theta_0+\psi_t) &(65)\\ \xi_{\mathcal{N}c} &= \eta\left|C_{\mathcal{N}}^t\right|\cos\left(\arg\{C_{\mathcal{N}}^t\}+\theta_0\right) &(66)\\ \xi_{\mathcal{N}s} &= \eta\left|C_{\mathcal{N}}^t\right|\sin\left(\arg\{C_{\mathcal{N}}^t\}+\theta_0\right) &(67)\\ \xi_{\mathcal{P}c} &= \eta\left|C_{\mathcal{P}}^t\right|\cos\left(\arg\{C_{\mathcal{P}}^t\}+\theta_0\right) &(68)\\ \xi_{\mathcal{P}s} &= \eta\left|C_{\mathcal{P}}^t\right|\sin\left(\arg\{C_{\mathcal{P}}^t\}+\theta_0\right) &(69)\end{aligned}$$

with the same method than for the backward case, the power spectral densities of the intensity, phase and carrier density noises are given by the following c_{ij} and d_{ij} coefficients and (48)

$$\begin{aligned}d_{11} &= -k_c - [\langle\xi_{\mathcal{N}c}\,|\,\Delta\mathcal{N}_0\rangle + \langle\xi_{\mathcal{P}c}\,|\,\Delta\mathcal{P}_0\rangle]\\ &\quad - \langle\xi_{\mathcal{P}c}|(1-\mathfrak{M}_{\mathcal{P}})^{-1}\,|2\mathcal{P}_0\rangle\\ &\quad - j\Omega\langle\xi_{\mathcal{P}c}|(1-\mathfrak{M}_{\mathcal{P}})^{-1}|H_I\rangle + \chi_s(\omega_i-\omega_s)\\ d_{12} &= -2I_0\{k_s + [\langle\xi_{\mathcal{N}s}\,|\,\Delta\mathcal{N}_0\rangle + \langle\xi_{\mathcal{P}s}\,|\,\Delta\mathcal{P}_0\rangle]\\ &\quad + j\Omega\langle\xi_{\mathcal{P}c}|(1-\mathfrak{M}_{\mathcal{P}})^{-1}|H_\phi\rangle + \chi_c(\omega_i-\omega_s)\}\\ d_{13} &= 2I_0\langle\xi_{\mathcal{N}c}| + 2I_0\langle\xi_{\mathcal{P}c}|\mathfrak{M}\\ d_{21} &= \frac{1}{2I_0}\Big\{k_s + [\langle\xi_{\mathcal{N}s}\,|\,\Delta\mathcal{N}_0\rangle + \langle\xi_{\mathcal{S}s}\,|\,\Delta\mathcal{P}_0\rangle]\\ &\quad - \langle\xi_{\mathcal{P}s}|(1-\mathfrak{M}_{\mathcal{P}})^{-1}|\mathcal{P}_0\rangle\\ &\quad - \frac{j\Omega}{2}\langle\xi_{\mathcal{P}s}|(1-\mathfrak{M}_{\mathcal{P}})^{-1}|H_I\rangle + \chi_c(\omega_i-\omega_s)\Big\}\\ d_{22} &= k_c + \langle\xi_{\mathcal{N}c}\,|\,\Delta\mathcal{N}_0\rangle + \langle\xi_{\mathcal{P}c}\,|\,\Delta\mathcal{P}_0\rangle\\ &\quad + j\Omega\langle\xi_{\mathcal{P}s}|(1-\mathfrak{M}_{\mathcal{P}})^{-1}|H_\phi\rangle - \chi_s(\omega_i-\omega_s)\\ d_{23} &= \langle\xi_{\mathcal{N}s}| + \langle\xi_{\mathcal{P}s}|\mathfrak{M} \qquad (70)\end{aligned}$$

$$\begin{aligned} c_{11} &= \frac{I_0}{I_{\text{in0}}}\{k_c + [\langle \xi_{\mathcal{N}c} \,|\, \Delta\mathcal{N}_0\rangle + \langle \xi_{\mathcal{P}c} \,|\, \Delta\mathcal{P}_0\rangle] \\ &\quad - \chi_s(\omega_i - \omega_s)\} + j\Omega\chi_c \\ c_{12} &= -2I_0\{k_s + [\langle \xi_{\mathcal{N}s} \,|\, \Delta\mathcal{N}_0\rangle + \langle \xi_{\mathcal{P}s} \,|\, \Delta\mathcal{P}_0\rangle] \\ &\quad + \chi_c(\omega_i - \omega_s) + j\Omega\chi_s\} \\ c_{21} &= \frac{1}{2I_{\text{in0}}}\{k_s + [\langle \xi_{\mathcal{N}s} \,|\, \Delta\mathcal{N}_0\rangle + \langle \xi_{\mathcal{P}s} \,|\, \Delta\mathcal{P}_0\rangle] \\ &\quad + \chi_c(\omega_i - \omega_s) + j\Omega\chi_s\} \\ c_{22} &= k_c + [\langle \xi_{\mathcal{N}c} \,|\, \Delta\mathcal{N}_0\rangle + \langle \xi_{\mathcal{P}c} \,|\, \Delta\mathcal{P}_0\rangle] \\ &\quad - \chi_s(\omega_i - \omega_s) + j\Omega\chi_c. \end{aligned} \tag{71}$$

E. Comments

In difference with the backward case, the coefficients c_{ij} and d_{ij}, depend on the structure of the laser. The coefficients m_{ij} remain identical to the backward case since they represent the noise properties of the laser without injection. It can be also noticed that all the coefficients c_{ij} and d_{ij}, excepted d_{13} and d_{23}, contain a component proportional to the frequency Ω. This contribution is particularly important for the characterization of the phase and intensity noise spectrum at large frequencies. For frequency closed to f_D, the Taylor expansion (16) and (54) should be extended to higher orders in $(\omega - \omega_s)$ leading to higher order temporal derivatives in (55) and polynomials in Ω instead of linear terms in the expression of c_{ij} and d_{ij}.

V. Application to Fabry–Pérot and DFB Lasers

A. Injection Locking of a Fabry-Pérot

We discuss in this section the application of the equations previously derived to a Fabry–Pérot cavity. The field is considered to be uniform along the cavity, the emission to be near the maximum of the gain curve and the gain compression to be negligible. These hypothesis are fulfilled with a Fabry–Pérot laser with facet reflectivities above 0.5, operating not too far from the threshold [64].

For the case of backward injection

$$f_D = \frac{1}{\tau_{\text{in}}} = \frac{v_g}{2l} \tag{72}$$

$$C_{\mathcal{N}} = \frac{1 + j\alpha_H}{2l} v_g \frac{\partial g}{\partial \mathcal{N}} \tag{73}$$

$$r_{Ls} = \frac{1}{r_2} \tag{74}$$

$$f_R = \frac{v_g}{2lr_2} \tag{75}$$

Consequently, from (19), the equation of motion of A^+ is

$$\begin{aligned} \frac{dA^+}{dt}(t) &= -j(\omega_s - \omega_i)A^+(t) \\ &\quad + \frac{1 + j\alpha_H}{2} v_g \frac{\partial g}{\partial \mathcal{N}} \Delta\mathcal{N}(t) A^+(t) \\ &\quad + \frac{v_g}{2l}\frac{t_{32}}{r_2} A^i(t) + F_A(t). \end{aligned} \tag{76}$$

This equation is similar to the well known equation used by Lang [16]. However, the feed-in rate used by Lang is $c/(2nl)$ whereas in our case the feed-in rate is $c/(2ln_g r_2)$. We can notice two differences, the use of the group index and the involvement of the facet reflectivity r_2. The phenomenological argument of Lang was that the injected field adds $t_{32}A_i$ every time it hits the irradiated facet at a time interval equal to the cavity round-trip time. However, the injected field is added only to the backward traveling wave reflected by the front facet with a coefficient of reflection r_2. Consequently when the forward traveling wave is considered, the feed-in rate is equal to the inverse of the round-trip time divided by r_2. In many papers on injection locking, the $1/r_2$ is missing. This problem is analog to the difference which has been noticed [65] between Kurokawa's [66] and Adler's [67] locking bandwidth due to the existence of different Q-factors, the resonator unloaded Q, the loaded Q and the external Q. The expression of the feed-in rate derived in [15] using the round-trip time travelling-wave amplifier model is equal to our expression. The expression of the feed-in rate given in [20] seems also to agree with our expression, however it is not clear whether it was established for the total intracavity electric field or for the forward traveling component. For the envelope of the total intracavity electric field at the front facet, the feed-in rate is $c(1+r_2)/(2ln_g r_2)$, it is in agreement with the value obtained in [28] which uses for the mirror the model of a dielectric plan where a surface current is induced by the electric field instead of the boundary conditions used in this article. In the forward case

$$t_{Ls} = \frac{1}{\sqrt{r_1 r_2}} \tag{77}$$

$$f_T = \frac{1}{\tau_{\text{in}}\sqrt{r_1 r_2}} \tag{78}$$

$$f_t = \frac{2}{\tau_{\text{in}}} \tag{79}$$

$$C^t_{\mathcal{N}} = -\frac{1 + j\alpha_H}{4l\sqrt{r_1 r_2}} \frac{\partial g}{\partial \mathcal{N}} v_g \tag{80}$$

and (55) becomes

$$\begin{aligned} \frac{dA^+}{dt}(t) &= j(\omega_s - \omega_i)A^+(t) + \frac{1 + j\alpha_H}{2} v_g \frac{\partial g}{\partial \mathcal{N}} \Delta\mathcal{N} A^+(t) \\ &\quad + \frac{t_{12}}{\tau_{\text{in}}\sqrt{r_1 r_2}} A^i(t) - \frac{(1 + j\alpha_H)t_{12}}{4\sqrt{r_1 r_2}} \frac{\partial g}{\partial \mathcal{N}} v_g \Delta\mathcal{N} A^i(t) \\ &\quad - j\frac{t_{12}}{2\sqrt{r_1 r_2}}(\omega_s - \omega_i)A^i(t) \\ &\quad + \frac{t_{12}}{2\sqrt{r_1 r_2}} \frac{d\,A^i}{dt}(t) + F_A(t). \end{aligned} \tag{81}$$

As previously noticed, the total feed-in rate can be decomposed in three terms, $\kappa_{\text{in}} = \kappa_{\text{in1}} + \kappa_{\text{in2}} + \kappa_{\text{in3}}$

$$\kappa_{\text{in1}} = \frac{1}{\tau_{\text{in}}\sqrt{r_1 r_2}} \tag{82}$$

$$\kappa_{\text{in2}} = -\frac{(1 + j\alpha_H)}{4\sqrt{r_1 r_2}} \frac{\partial g}{\partial \mathcal{N}} v_g \Delta\mathcal{N} \tag{83}$$

$$\kappa_{\text{in3}} = -j\frac{\omega_s - \omega_i}{2\sqrt{r_1 r_2}}. \tag{84}$$

κ_{in1} is the main term of κ_{in}. It is identical to the backward case only for a symmetric laser. The others terms of κ_{in} can become noticeable when the cavity is particularly long or when locking is achieved with very large detuning. Finally, the contribution of the derivative of the envelope of the injected electric field can become noticeable when the variation of A^i during a round-trip time is nonnegligible, for example when the master laser is modulated at high frequency which is an important point in telecommunication applications.

B. Numerical Applications for DFB Laser With an Antireflection Coating

We will now present numerical results for the parameters f_R, f_T χ_t for DFB lasers with an antireflection coated front facet.

1) Parameters of Injection of a DFB Laser With an Antireflection Coated Facet: For the Fabry–Pérot cavity, f_D represents the inverse of the round-trip time of the wave between the two reflective facets. However, in a DFB laser, the definition of the round-trip time is not straightforward due to the distributed reflection added to the facet reflections. Consequently $1/f_D$ represents an effective round-trip time for a laser containing distributed reflections. The resolution of the coupled equations for a DFB laser [56] with coupling coefficient of the grating κ, Bragg wave number β_B and grating phase Ω_B gives

$$r_L = \frac{(\kappa + \delta\rho_1)\tanh(\gamma l) + j\gamma\rho_1}{-(\kappa\rho_1 + \delta)\tanh(\gamma l) + j\gamma} e^{-j\Omega} \tag{85}$$

with $\delta = k - \beta_B$, the complex detuning from the Bragg wave number, $\rho_1 = r_1 e^{j(\Omega_B - 2\beta_B l)}$ and $\gamma = \sqrt{\kappa^2 - \delta^2}$, the complex wave number of the longitudinal envelope. For an antireflection coated front facet laser, the resonance condition is $1/r_{Ls} = 0$, consequently

$$\tanh(\gamma l) = \frac{j\gamma}{\kappa\rho_1 + \delta}. \tag{86}$$

The expression of f_R is calculated from (85) and (86)

$$f_R = -j\frac{v_g}{l}\frac{[(\kappa l)^2 - (\gamma l)^2]\left[(1+\rho_1^2) + 2\rho_1\frac{\gamma}{\kappa}\right]}{(\gamma l)\left[\rho_1 + j(\kappa l)(1+\rho_1^2)\right] + \kappa l + 2j\rho_1(\gamma l)^2}. \tag{87}$$

For forward injection, the additional parameter f_t is derived from t_L/r_L, calculated from the solution of the coupled equations

$$\frac{t_L}{r_L} = \frac{\gamma e^{j\beta_B l}}{-j\kappa^* e^{-j\Omega}\sinh(\gamma l) + r_1[\cosh(\gamma l) - j\delta\sinh(\gamma l)]}. \tag{88}$$

We will now present numerical results for the parameter of injection in forward and backward configuration.

2) Case of a Real Rear Reflectivity: Fig. 2 (left) shows the modulus of the feed-in rate f_R as a function of the normalized coupling coefficient of the grating $\kappa \cdot l$ for four different values of the rear facet reflectivity. The feed-in rate is normalized by the free spectral range of a Fabry–Pérot laser of the same length. The normalized values of the feed-in rate are distributed around two curves. The higher curve corresponds to a wavelength lower than the Bragg wavelength, whereas the lower curve corresponds to a higher wavelength. The discontinuity for $r_1 = 0.565$, $\kappa.l = 1.75$ and $r_1 = 0.775$, $\kappa.l = 3.25$ are due to a mode hopping corresponding to a change of the sign of the detuning from the Bragg frequency. The normalized value of the feed-in rate for a cleaved facet Fabry–Pérot laser $(r = -0.565)$ is 1.8. Consequently, for normalized coupling coefficients of the grating lower than 1.5, the feed-in rate of the DFB laser is higher than for a Fabry–Pérot laser, in the limit of a rear facet reflectivity lower than 0.95. For higher coupling coefficient of the grating and intermediate values of the rear facet reflectivity, the feed-in rate of the DFB is lower than for a Fabry–Pérot laser. For strong coupling the influence of the boundary conditions is weaker due to the predominance of the distributed reflection, and consequently the feed-in rate is weaker. Moreover the feed-in rate tends toward zero for very high coupling coefficients regardless of the rear reflectivity. In contrast, for weak coupling, the value of the rear reflectivity and the position of the lasing wavelength have an important influence on the feed-in rate.

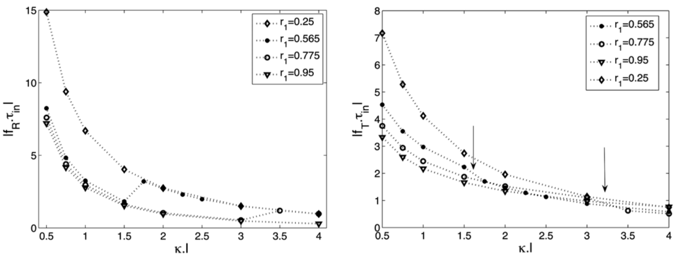

Fig. 2. Normalized feed-in rate for the backward injection (left) and forward injection (right).

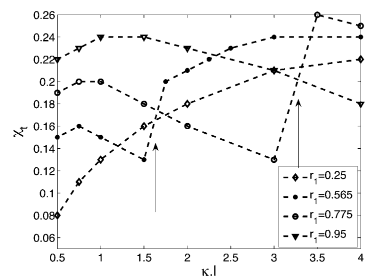

Fig. 3. χ_t as a function of the coupling coefficient of the grating.

On Fig. 2 (right) are shown the normalized modulus of the primary feed-in rate (f_T) for forward injection as a function of the normalized coupling coefficient to the grating and for four different values of the reflectivity of the rear facet. For a cleaved facet Fabry–Pérot laser, the normalized feed-in rate is equal to 1.8. Consequently, the primary feed-in rate of the DFB laser becomes lower than for a Fabry–Pérot laser for coupling coefficients higher than 1.7. The effect of the mode hopping for $r_1 = 0.775$ and 0.565 is indicated by the two arrows and is weaker than for the backward case.

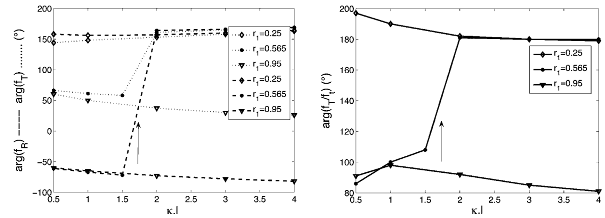

Fig. 4. Argument of the feed in rate for the backward and forward injection (left) and phase shift between f_T and f_t (right).

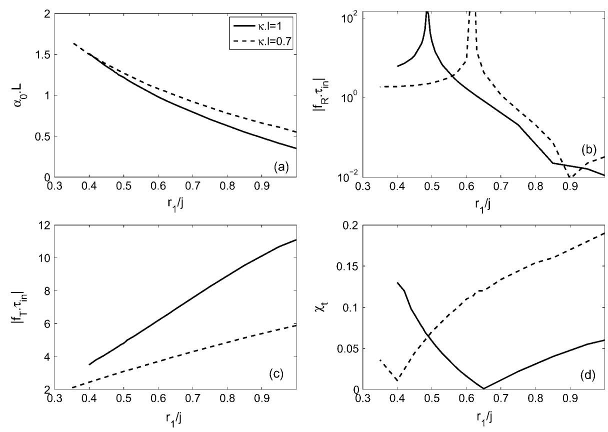

Fig. 5. Parameters as a function of the reflectivity for two different coefficients (a) threshold gain, (b) forward feed-in rate, (c) backward feed-in rate, and (d) χ_t forward parameter.

On Fig. 3 are represented the parameter χ_t specific to the forward injection as a function of the normalized coefficient of the grating and for four different rear reflectivities. We notice than the values do not exhibit the same decay curve as in the case of f_R and f_T. For a wavelength lower than the Bragg wavelength ($r_1 = 0.95$, $r_1 = 0.775$, and $\kappa \cdot l > 1.7$, $r_1 = 0.565$, and $\kappa.l > 3.2$), χ_t increases with $\kappa.l$ and for a wavelength higher ($r_1 = 0.25, r_1 = 0.775$, and $\kappa \cdot l < 1.7$, $r_1 = 0.565$ and $\kappa \cdot l < 3.2$) it decreases. The value of χ_t for a cleaved facet Fabry–Pérot is 0.9, consequently the additional coupling measured by χ_t is weaker in a DFB laser than in a Fabry–Pérot laser.

Finally, Fig. 4 presents the arguments of f_R, f_T and f_T/f_t in degrees as a function of the normalized coupling coefficient of the grating for three different values of the rear reflectivity. The change of position of the mode indicated by the arrow is associated to a phase rotation of nearly 180° of f_R and 90° of f_T. Arguments of f_T/f_t exhibits a behavior similar to the argument of f_R.

3) Lasing Mode in the Forbidden Band: We have previously studied the case of a DFB laser with an antireflection coated front facet and a rear facet with a real reflectivity. The case of a purely imaginary rear reflectivity is also interesting because in this case the principal mode of the laser is in the center of the forbidden band [17].

In Fig. 5 are shown (a) the normalized threshold gain α_0, (b)–(c) the normalized modulus of the feed-in rates f_R, f_T, and (d) the parameter χ_t, as a function of the modulus of the rear reflectivity. Only the reflectivities for which the Bragg mode has the lowest threshold have been considered. Two coupling coefficients of the grating have been used, $\kappa \cdot l = 1$ and $\kappa \cdot l = 0.7$. The value of f_R strongly varies with the reflectivity and becomes extremely high for $r_1 = j0.487(\kappa \cdot l = 1)$ and $r_1 = j0.62(\kappa \cdot l = 0.7)$. By comparison, Fig. 2(left) presents, for real reflectivities, ranges of normalized value of the module of the feed-in rate of [4.5, 9.5] for $\kappa \cdot l = 0.7$, and [2.7, 7] for $\kappa \cdot l = 1$. For high values of r_1, the feed-in rate is practically two orders of magnitude below the feed-in rate of the cleaved facet Fabry–Pérot laser. These results are important since they demonstrate that in choosing appropriately the value of the rear reflectivity, the feed-in rate, and consequently the locking range, can become extremely high or extremely small.

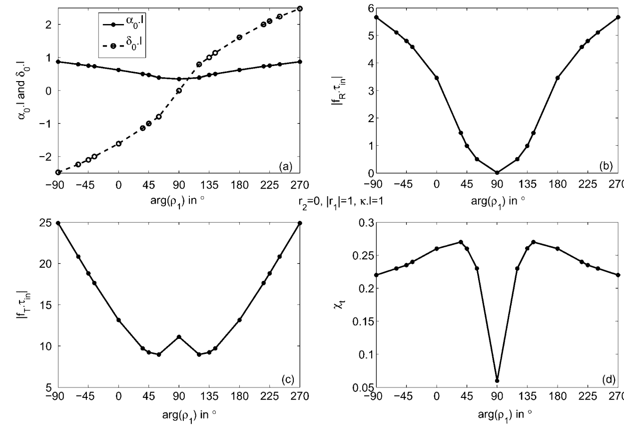

Fig. 6. Influence of the phase of the reflectivity on the parameter of injection (a) threshold gain and Bragg detuning, (b) forward feed-in rate, (c) backward feed-in rate, and (d) χ_t forward parameter.

We do not find the same large range of values for the primary feed-in rate f_R in the forward injection. However Fig. 5 shows that it increases with the reflectivity which is inverse to the case of a real reflectivity. Moreover, the sensitivity to the coupling coefficient of the grating is higher.

Finally, the results presented for the parameter χ_t exhibit, as for the real reflectivity case, values lower than for the cleaved facet Fabry–Pérot laser. It is interesting to note that for every value of $\kappa \cdot l$, there is a value of r_1 for which χ_t is zero.

4) Influence of the Phase of the Coefficient of Reflection: We have shown that results for real and purely imaginary reflectivity are strongly different. Consequently we will now study the impact of the argument of the rear reflectivity on the different parameters considered.

In Fig. 6 are shown (a) the normalized Bragg detuning and threshold gain, (b) the modulus of the normalized feed-in rate f_R for backward injection, (c) the modulus of the normalized primary feed-in rate f_T, and (d) the parameter χ_t for forward injection, all as a function of the argument of the rear reflectivity. The results concerning the feed-in rate f_R show that it has a quadratic behavior centered around the case of the Bragg mode ($\pi/2$). Consequently the influence of the argument is particularly important near the real axis. For the forward injection, the Bragg mode corresponds to a local maximum of f_T. A phase shift of 45° from the imaginary axis induces a decrease of the primary feed-in rate of 30%. Between 45° and $-90°$ and between 135° and 270°, f_T depends quasi-linearly on the argument of the reflectivity. Finally, the Bragg mode corresponds to a minimum for the parameter χ_t. In opposition with f_R, the Bragg mode is the case where the influence of the argument of the reflectivity is the highest. Once again, all the values of χ_t presented are below the case of the cleaved facet Fabry–Pérot cavity.

VI. Conclusion

We have presented a theory for the injection locking of multisection lasers taking into account spatial hole burning, the nonlinear gain and the direction of injection. The contribution of the spontaneous emission has been treated with the Green's function method and the contribution of the injected fields using effective reflection and transmission coefficients accounting for longitudinal distribution of the carrier and photon densities. Two different equations of evolution for the complex envelope of the forward component of the intracavity electric field at the front facet have been derived, corresponding to the two possible directions of injection. This analysis shows that backward injection corresponds to the classical equation of Lang, whereas forward injection leads to additional contributions. Part of those additional contributions has been previously found in the equation derived by Tromborg *et al.* [31], but the contribution of the detuning was missing and it was not pointed out that those contributions were related to the facet of injection. The paper provides analytical expressions of the noise power spectral densities including mathematical tools presented in [47]. Those expressions are interesting for accurate characterization of the phase noise spectrum of injection-locked laser, especially for forward injection and for injection of modulated light. Moreover, they show that injection-locked lasers can exhibit asymmetric noise properties, which has been experimentally demonstrated in laser submitted to external feedback [68]. The application of our general equation to Fabry–Pérot laser shows that the expression of the feed-in rate considered in the literature is sometimes incomplete. Finally, numerical results demonstrate the possibility of designing DFB lasers with very large feed-in rate for backward injection, and DFB lasers with significantly different feed-in rate for forward and backward injection.

Appendix A
Resolution of the Inhomogeneous Helmholtz Equation With Green's Function

Knowing two independent solutions Z_1 et Z_2 of the homogeneous Helmholtz equation, i.e., two solutions with Wronskian

$$W = Z_1 dZ_2/dz - Z_2 dZ_1/dz \tag{89}$$

different from zero, the general solution of the inhomogeneous equation can be expressed as

$$E(z,\omega) = Z_0(z) + \int_z^l f(z,\omega') \frac{[Z_1(z)Z_2(z') - Z_2(z)Z_1(z')]}{W} dz' \tag{90}$$

with Z_0 is a solution of the homogeneous equation determined by the boundary conditions

$$E^+(0^+,\omega) = r_1 E^-(0^+,\omega) + t_{12} E^+_{\text{injL}}(0^-,\omega) \tag{91}$$
$$E^-(l^-,\omega) = r_2 E^+(l^-,\omega) + t_{32} E^-_{\text{inj}R}(l^+,\omega). \tag{92}$$

$E^+_{\text{injL}}(0^-,\omega)$ and $E^-_{\text{inj}R}(l^+,\omega)$ are the projection of the external field on the transverse mode and polarization vector of the cavity in, respectively, 0^- and l^+

$$E_{\text{inj}}(z,\omega) = \frac{\int\int \vec{E}_{\text{ext}}(x,y,z,\omega)\Phi(x,y)\vec{u}\,dx\,dy}{\int\int \Phi(x,y)\Phi(x,y)\,dx\,dy}. \tag{93}$$

We choose Z_2 satisfying the left boundary condition without injection. Consequently, the left boundary condition gives

$$\begin{aligned} Z_0^+(0) - r_1 Z_0^-(0) &= (r_1 Z_1^-(0) - Z_1^+(0)) \int_0^l f(\omega,z') \frac{Z_2(z')}{W} dz' \\ &\quad + t_{12} E^+_{\text{injL}}(0^-). \end{aligned} \tag{94}$$

If Z_1 satisfies $Z_1(0) = 0$ and $dZ_1(0)/dz = 1$ such that $W = (1+r_1)Z_2^-(0)$, since Z_0 is a solution of the homogeneous equation, Z_2 satisfies the left boundary condition and $E(l^-,\omega) = Z_0(l)$

$$\begin{aligned} Z_0^+(l)Z_2^+(l) - Z_0^-(l)Z_2^-(l) &= Z_1^+(0) \int_0^l f(\omega,z') \frac{Z_2(z')}{W} dz' \\ &\quad + Z_2^-(0) t_{12} E^+_{\text{injL}}(0^-). \end{aligned} \tag{95}$$

Using now the right boundary condition and defining the reflectivity r_L and the transmission coefficient t_L

$$r_L = Z_L^+(l^-)/Z_L^-(l^-) \tag{96}$$
$$t_L = Z_L^+(0^+)/Z_L^-(l^-) \tag{97}$$
$$F_L(\omega) = \frac{Z_1^+(0)}{Z_L^-(l)} \int_0^l f(z',\omega) Z_L(z') dz' \tag{98}$$

we obtain the following equation for $E^+(l^-,\omega)$:

$$\begin{aligned} E^+(l^-,\omega) &= r_2 r_L E^+(l^-,\omega) + t_L t_{12} E^+_{\text{injL}}(0^-,\omega) \\ &\quad + r_L t_{32} E^-_{\text{inj}R}(l^+,\omega) + F_L(\omega). \end{aligned} \tag{99}$$

APPENDIX B EXPRESSION OF THE PHOTON LONGITUDINAL DENSITY

Equation (44) is the expansion of the photon density established by Tromborg *et al.* [47]. In this appendix, we briefly remind the method and the expression of the main parameters. The longitudinal mode is expended at first-order in ω, $\mathcal{P}$ and $\mathcal{N}$

$$Z_L(z) = Z_{L0}(z)+\frac{\partial Z_L}{\partial \omega}(\omega-\omega_s)+\langle Z_{\mathcal{N}}(z)\,|\,\delta\mathcal{N}\rangle+\langle Z_{\mathcal{P}}(z)\,|\,\delta\mathcal{P}\rangle \tag{100}$$

with

$$\frac{\delta Z_L(z)}{\delta k(z')}\frac{\partial k_0}{\partial \mathcal{N}} = Z_{\mathcal{N}}(z,z') \tag{101}$$

$$\frac{\delta Z_L(z)}{\delta k(z')}\frac{\partial k_0}{\partial \mathcal{P}} = Z_{\mathcal{P}}(z,z') \tag{102}$$

$Z_{L0}(z)$ is the stationary longitudinal mode with injection. Using (13) and Fourier transform, we obtain

$$|\delta\mathcal{P}\rangle = \mathfrak{M}_{\mathcal{N}}|\delta\mathcal{N}\rangle+\mathfrak{M}_{\mathcal{P}}|\delta\mathcal{P}\rangle+\left[|\mathcal{P}_0\rangle\frac{\delta I}{I_0}+\frac{|H_I\rangle}{2I_0}\frac{d\delta I}{dt}+|H_\phi\rangle\frac{d\phi}{dt}\right] \tag{103}$$

where two operators are defined

$$\mathfrak{M}_{\mathcal{P}} = \frac{2\Re e\{Z_{L0}(z)\}}{|Z_{LO}(z)|^2}|\mathcal{P}_0\rangle\langle Z_{\mathcal{P}}(z)| \tag{104}$$

$$\mathfrak{M}_{\mathcal{N}} = \frac{2\Re e\{Z_{L0}(z)\}}{|Z_{LO}(z)|^2}|S_0\rangle\langle Z_{\mathcal{N}}(z)|. \tag{105}$$

Finally, supposing $1-\mathfrak{M}_{\mathcal{P}}$ invertible and noting

$$\mathfrak{M} = (1-\mathfrak{M}_{\mathcal{P}})^{-1}\mathfrak{M}_{\mathcal{N}} \tag{106}$$

we obtain [47]

$$|\delta P\rangle = (1-\mathfrak{M}_{\mathcal{P}})^{-1}\times\left[|\mathcal{P}_0\rangle\frac{\delta I}{I_0}+\frac{|H_I\rangle}{2I_0}\frac{d\delta I}{dt}+|H_\phi\rangle\frac{d\phi}{dt}\right] + \mathfrak{M}|\delta\mathcal{N}\rangle. \tag{107}$$

$H_\phi(z)$ and $H_I(z)$ come from the ω dependance of Z_L

$$H_\phi(z) = 2\Re e\left\{I_0 Z_{L0}^*(z)\frac{\partial Z_L}{\partial \omega}(z,\omega_s)\right\} \tag{108}$$

$$H_I(z) = 2\Im m\left\{I_0 Z_{L0}^*(z)\frac{\partial Z_L}{\partial \omega}(z,\omega_s)\right\}. \tag{109}$$

REFERENCES

[1] S. Kobayashi, Y. Yamamoto, and T. Kimura, "Optical FM signal amplification and FM noise-reduction in an injection locked AlGaAs semiconductor laser," *Electron. Lett.*, vol. 17, no. 22, pp. 849–851, 1981.

[2] K. Kikuchi, C.-E. Zah, and T. Lee, "Amplitude-modulation sideband injection locking characteristics of semiconductor lasers and their application," *J. Lightw. Technol.*, vol. 6, no. 12, pp. 1821–1830, Dec. 1988.

[3] T. B. Simpson, J. M. Liu, and G. A. , "Bandwidth enhancement and broadband noise reduction in injection-locked semiconductor lasers," *IEEE Photon. Technol. Lett.*, vol. 7, no. 7, pp. 709–711, 1995.

[4] L. A. Johansson and A. J. Seeds, "Millimeter-wave modulated optical signal generation with high spectral purity and wide-locking bandwidth using a fiber-integrated optical injection phase-lock loop," *IEEE Photon. Technol. Lett.*, vol. 12, no. 6, pp. 690–692, Jun. 2000.

[5] C. W. Chow, C. S. Wong, and H. K. Tsang, "All-optical modulation format conversion and multicasting using injection-locked laser diodes," *J. Lightw. Technol.*, vol. 22, no. 11, pp. 2386–2392, Nov. 2004.

[6] H. Wang, M. J. Freeman, and D. G. Steel, "Squeezed light from injection-locked quantum well lasers," *Phys. Rev. Lett.*, vol. 71, no. 24, pp. 3951–3954, 1993.

[7] J. Jahanpanah and R. Loudon, "Theory of laser-amplifier injection locking," *Phys. Rev. A*, vol. 54, no. 6, pp. 5210–5226, 1996.

[8] A. Murakami and J. Ohtsubo, "Synchronization of feedback-induced chaos in semiconductor lasers by optical injection," *Phys. Rev. A*, vol. 65, no. 3, p. 033826, 2002.

[9] D. Goulding, S. P. Hegarty, O. Rasskazov, S. Melnik, M. Hartnett, G. Greene, J. G. McInerney, D. Rachinskii, and G. Huyet, "Excitability in a quantum dot semiconductor laser with optical injection," *Phys. Rev. Lett.*, vol. 98, no. 15, p. 153903, 2007.

[10] J. M. Liu and T. B. Simpson, "Characterization of fundamental parameters of a semiconductor laser with an injected optical probe," *IEEE Photon. Technol. Lett.*, vol. 5, no. 4, pp. 380–382, Apr. 1993.

[11] M. P. van Exter, C. Biever, and J. P. Woerdman, "Effect of optical injection on bias voltage and spectrum of a semiconductor laser," *IEEE J. Quantum Electron.*, vol. 29, no. 11, pp. 2771–2779, Nov. 1993.

[12] H. L. Stover and W. Steier, "Locking of laser oscillators by light injection," *Appl. Phys. Lett.*, vol. 8, pp. 91–93, Aug. 1966.

[13] S. Kobayashi and T. Kimura, "Injection locking in AlGaAs semiconductor laser," *IEEE J. Quantum Electron.*, vol. 17, no. QE-5, pp. 681–689, May 1981.

[14] K. Otsuka and S. Tarucha, "Theoretical studies on injection locking and injection-induced modulation of laser diodes," *IEEE J. Quantum Electron.*, vol. QE–17, no. 8, pp. 1515–1521, Aug. 1981.

[15] G. H. M. van Tartwijk and D. Lenstra, "Semiconductor lasers with optical injection and feedback," *Quantum Semiclass. Opt.*, vol. 7, no. 2, pp. 87–143, 1995.

[16] R. Lang, "Injection locking properties of a semiconductor laser," *IEEE J. Quantum Electron.*, vol. QE-18, no. 6, pp. 976–983, Jun. 1982.

[17] C. H. Henry, N. A. Olsson, and N. K. Dutta, "Locking range and stability of injection locked 1.54 μm InGaAsP," *IEEE J. Quantum Electron.*, vol. QE-21, no. 8, pp. 1152–1156, Aug. 1985.

[18] F. Mogensen, H. Olesen, and G. Jacobsen, "Locking conditions and stability properties for a semiconductor laser with external light injection," *IEEE J. Quantum Electron.*, vol. QE-21, no. 7, pp. 784–793, Jul. 1985.

[19] P. Gallion, H. Nakajima, G. Debarge, and C. Chabran, "Contribution of spontaneous emission to the linewidth of an injection-locked semiconductor laser," *Electron. Lett.*, vol. 21, no. 14, pp. 626–628, 1985.

[20] N. Schunk and K. Petermann, "Noise analysis of injection-locked semiconductor injection lasers," *IEEE J. Quantum Electron.*, vol. QE-22, no. 5, pp. 642–650, May 1986.

[21] P. Spano, S. Piazzolla, and M. Tamburrini, "Frequency and intensity noise in injection-locked semiconductor lasers: Theory and experiments," *IEEE J. Quantum Electron.*, vol. QE-22, no. 3, pp. 427–435, Mar. 1986.

[22] I. Petitbon, P. Gallion, G. Debarge, and C. Chabran, "Locking bandwidth and relaxation oscillations of an injection-locked semiconductor laser," *IEEE J. Quantum Electron.*, vol. 24, no. 4, pp. 148–154, Apr. 1988.

[23] O. Lidoyne, P. B. Gallion, and D. Erasme, "Modulation properties of an injection-locked semiconductor laser," *IEEE J. Quantum Electron.*, vol. 27, no. 3, pp. 344–351, Mar. 1991.

[24] J. Wang, M. K. Haldar, L. Li, and F. Mendis, "Enhancement of modulation bandwidth of laser diodes by injection locking," *IEEE Photon. Technol. Lett.*, vol. 8, no. 1, pp. 34–36, Jan. 1996.
[25] S. Wieczorek, W. W. Chow, L. Chrostowski, and C. J. Chang-Hasnain, "Improved semiconductor-laser dynamics from induced population pulsation," *IEEE J. Quantum Electron.*, vol. 42, no. 5, pp. 552–562, May 2006.
[26] L. Li, "Static and dynamic properties of injection-locked semiconductor lasers," *IEEE J. Quantum Electron.*, vol. 30, no. 8, pp. 1701–1708, Aug. 1994.
[27] O. Lidoyne, P. Gallion, C. Chabran, and G. Debarge, "Locking range, phase noise and power spectrum of an injection-locked semiconductor laser," *Proc. IEE*, vol. 137, no. J3, pp. 147–154, 1990.
[28] M. B. Spencer and W. E. Lamb, Jr., "Laser with a transmitting window," *Phys. Rev. A*, vol. 5, no. 2, pp. 884–892, 1972.
[29] G. R. Hadley, "Injection locking of diode lasers," *IEEE J. Quantum Electron.*, vol. QE-22, no. 3, pp. 419–426, mar. 1986.
[30] F. Favre, "Theoretical analysis of external optical feedback on DFB semiconductor lasers," *IEEE J. Quantum Electron.*, vol. QE-23, no. 1, pp. 81–88, Jan. 1987.
[31] B. Tromborg, H. Olesen, X. Pan, and S. Saito, "Transmission line description of optical feedback and injection locking for Fabry–Pérot and DFB lasers," *IEEE J. Quantum Electron.*, vol. 23, no. 11, pp. 1875–1889, Nov. 1987.
[32] R. Hui, A. D'Ottavi, A. Mecozzi, and P. Spano, "Injection locking in distributed feedback semiconductor lasers," *IEEE J. Quantum Electron.*, vol. 27, no. 6, pp. 1688–1695, Jun. 1991.
[33] J.-P. Bouyer and C. Bréant, "Stability of an injection-locked DFB 1.5 μm semiconductor laser," *J. Physique III*, vol. 9, pp. 1623–1644, 1992.
[34] J. Troger, P.-A. Nicati, L. Thévenaz, and P. A. Robert, "Novel measurement scheme for injection-locking experiments," *IEEE J. Quantum Electron.*, vol. 25, no. 6, pp. 1254–1260, Jun. 1989.
[35] P. Vankwikelberge, G. Morthier, and R. Baets, "CLADISS—A longitudinal multimode model for the analysis of the static, dynamic, and stochastic behavior of diode lasers with distributed feedback," *IEEE J. Quantum Electron.*, vol. 26, no. 10, pp. 1728–1741, Oct. 1990.
[36] S. Hansmann, "Transfer matrix analysis of the spectral properties of complex distributed feedback laser structures," *IEEE J. Quantum Electron.*, vol. 28, no. 11, pp. 2589–2595, Nov. 1992.
[37] O. Hess and T. Kuhn, "Maxwell-Bloch equations for spatially inhomogeneous semiconductor lasers. I. Theoretical formulation," *Phys. Rev. A*, vol. 54, no. 4, pp. 3347–3359, 1996.
[38] O. Hess and T. Kuhn, "Maxwell-Bloch equations for spatially inhomogeneous semiconductor lasers. II. Spatiotemporal dynamics," *Phys. Rev. A*, vol. 54, no. 4, pp. 3360–3368, 1996.
[39] M. Radzianus, H.-J. Wunsche, B. Sartorius, O. Brox, D. Hoffmann, K. Schneider, and D. Marcenac, "Modeling self-pulsating DFB lasers with an integrated phase tuning section," *IEEE J. Quantum Electron.*, vol. 36, no. 9, pp. 1026–1034, Sep. 2000.
[40] U. Bandelow, M. Radziunas, J. Sieber, and M. Wolfrum, "Impact of gain dispersion on the spatio-temporal dynamics of multisection lasers," *IEEE J. Quantum Electron.*, vol. 37, no. 2, pp. 183–188, Feb. 2001.
[41] C. H. Henry, "Theory of spontaneous emission noise in open resonators and its application to lasers and optical amplifiers," *J. Lightw. Technol.*, vol. 4, no. 3, pp. 288–297, mar. 1986.
[42] T. Makino, "Transfer-matrix analysis of the intensity and phase noise of multisection DFB semiconductor lasers," *IEEE J. Quantum Electron.*, vol. 27, no. 11, pp. 2404–2414, Nov. 1991.
[43] R. Marani and M. Lax, "Spontaneous emission in nonhermitian optical-systems—distributed-feedback semiconductor-lasers," *Phys. Rev. A*, vol. 52, no. 3, pp. 2376–2387, 1995.
[44] M. F. Peirera, Jr. and K. Henneberger, "Green's functions theory for semiconductor-quantum-well laser spectra," *Phys. Rev. B*, vol. 53, no. 24, pp. 16 485–16 496, 1996.
[45] H. Wenzel, "Green's function based simulation of the optical spectrum of multisection lasers," *IEEE J. Sel. Topics Quantum Electron.*, vol. 9, no. 3, pp. 865–871, May/Jun. 2003.
[46] R. Loudon, D. Ramoo, and M. J. Adams, "Theory of spontaneous emission noise in multisection semiconductor lasers," *J. Lightw. Technol.*, vol. 23, no. 8, pp. 2491–2504, Aug. 2006.
[47] B. Tromborg, H. Olesen, and X. Pan, "Theory of linewidth for multielectrode laser diodes with spatially distributed noise sources," *IEEE J. Quantum Electron.*, vol. 27, no. 2, pp. 178–192, Feb. 1991.
[48] X. Pan, H. Olesen, and B. Tromborg, "Modulation characteristics of tunable DFB/DBR lasers with one or two passive tuning sections," *IEEE J. Quantum Electron.*, vol. 25, no. 6, pp. 1254–1260, Jun. 1989.
[49] H. Olesen, B. Tromborg, X. Pan, and H. E. Lassen, "Stability and dynamic properties of multi-electrode laser diodes using Green's function approach," *IEEE J. Quantum Electron.*, vol. 29, no. 8, pp. 2282–2301, Aug. 1993.
[50] C. H. Chen and G. Griffel, "Static, dynamic, and noise analysis of multisection DFB lasers using frequency-domain transmission line model," *IEEE J. Quantum Electron.*, vol. 34, no. 9, pp. 1533–1544, Sep. 1998.
[51] B. Tromborg and J. Mørk, "Nonlinear injection locking dynamics and the onset of coherence collapse in external cavity lasers," *IEEE J. Quantum Electron.*, vol. 26, no. 4, pp. 642–654, Apr. 1990.
[52] G.-H. Duan, P. Gallion, and G. P. Agrawal, "Dynamic and noise properties of tunable multielectrode semiconductor lasers including spatial hole burning and nonlinear gain," *IEEE J. Quantum Electron.*, vol. 29, no. 3, pp. 844–854, Mar. 1993.
[53] F. Grillot, B. Thedrez, and G.-H. Duan, "Feedback sensitivity and coherence collapse threshold of semiconductor dfb lasers with complex structures," *IEEE J. Quantum Electron.*, vol. 40, no. 3, pp. 231–240, Mar. 2004.
[54] E. Detoma, B. Tromborg, and I. Montrosset, "The complex way to laser diode spectra: Example of an external cavity laser strong optical feedback," *IEEE J. Quantum Electron.*, vol. 41, no. 2, pp. 171–182, Feb. 2005.
[55] L. D. Landau and E. M. Lifshitz, *Statistical Physics*. London, U.K.: Addison Wesley, 1969.
[56] G. P. Agrawal and N. K. Dutta, *Semiconductors Lasers*. New York: Van Nostrand Reinhold, 1993.
[57] X. Pan, H. Olesen, and B. Tromborg, "Spectral linewidth of DFB lasers including the effects of spatial holeburning and nonuniform current injection," *IEEE Photon. Technol. Lett.*, vol. 2, no. 5, pp. 312–315, May 1990.
[58] G. P. Agrawal, "Gain nonlinearities in semiconductor lasers: Theory and application to distributed feedback lasers," *IEEE J. Quantum Electron.*, vol. 23, no. 6, pp. 860–868, Jun 1987.
[59] K. Petermann, "Calculated spontaneous emission factor for double-heterostructure injection lasers with gain-induced waveguiding," *IEEE J. Quantum Electron.*, vol. QE-15, no. 7, pp. 566–570, Jul. 1979.
[60] C. Henry and R. F. Kazarinov, "Quantum noise in photonics," *Rev. Mod. Phys.*, vol. 68, no. 3, pp. 802–851, 1996.
[61] M. Lax, "Classical noise IV:Langevin methods," *Rev. Mod. Phys.*, vol. 38, pp. 541–566, 1966.
[62] J. Genest, M. Chamberland, P. Tremblay, and M. Têtu, "Microwave signals generated by optical heterodyne between injection-locked semiconductor lasers," *IEEE J. Quantum Electron.*, vol. 33, no. 6, pp. 989–998, Jun. 1997.
[63] P. Spano, S. Piazzolla, and M. Tamburrini, "Phase noise in semiconductor lasers: A theoretical approach," *IEEE J. Quantum Electron.*, vol. 19, no. 7, pp. 1195–1199, Jul. 1994.
[64] B. J. Thedrez and C. H. Lee, "Reassessment of standard rate equations for low facet reflectivity semiconductor lasers using traveling wave rate equations," *IEEE J. Quantum Electron.*, vol. 28, no. 12, pp. 2706–2713, Dec. 1992.
[65] X. Wang and N. J. Gomes, "Locking bandwidth equations for electrically and optically injection-locked oscillators," *Proc. IEE Optoelectron.*, vol. 151, no. 6, pp. 476–481, 2004.
[66] K. Kurokawa, "Noise in synchronized oscillators," *IEEE Trans. Microw. Theory Tech.*, vol. MTT-16, no. 4, pp. 234–240, Apr. 1968.
[67] R. Adler, "A study of locking phenomena in oscillators," in *Proc. IRE*, 1946, vol. 34, pp. 351–356.
[68] J. Mink and B. H. Verbeek, "Asymetric noise and output power in semiconductor lasers with optical feedback near threshold," *Appl. Phys. Lett.*, vol. 48, no. 12, pp. 745–747, 1986.

Fabien Kéfélian was born in 1979. He received the Diplôme d'Ingénieur of the École Supérieure d'Optique, Orsay, France, in 2002, the Diplôme d'Études Approfondies in optics and photonics from the Université Paris-XI, Orsay, France, in 2002, and the doctor's degree in quantum electronics and optical communications from the École Nationale Supérieure des Télécommunications (ENST), Paris, France, in 2005.

From 2002 to 2005, he was with the Département Communications et Électronique of ENST carrying out research on injection locking, optical noise, DFB lasers and radio-over-fiber. After completion of his doctorate, he worked on multisection laser modeling in III–V Laboratory, Alcatel, Palaiseau, France, and joined in July 2006 the Tyndall National Institute, Cork, Ireland, where he worked on mode-locking and quantum-dot lasers. Since October 2007 he has been with the Laboratoire de Physique des Lasers, Université Paris-XIII, Villetaneuse, France, where he is involved in transmission of ultrastable optical frequencies on optical fiber.

Philippe Gallion (M'82–SM'93) received the Doctorat de Troisième Cycle from the University of Rheims, Rheims, France, in 1975 and the Doctorat d'Etat from the University of Montpellier, Montpellier, France, in 1986.

In 1978, he joined the Ecole Nationale Supérieure des Télécommunications (ENST) also called Télécom Paris, where he is presently full Professor. He is carrying out research at the Laboratoire de Traitement et Communication de l'Information (LTCI), joint research laboratories between ENST and the Centre National de la Recherche Scientifique (CNRS), where he is in charge of research activities in the fields of communications, electronics, radiofrequencies and optoelectronics. He has made pioneering contributions on laser noise, injection locking, semiconductor laser modulation chirp and tuning, coherent systems and optical devices, digital optical communications systems and networks. His present research topics include theory, design, modeling and characterization of functional devices, advanced optical digital communication systems and networks, radio over fiber systems and quantum cryptography systems. He is author or coauthor of more than 200 technical papers and communications and he has served as advisor for more than 40 Ph.D. degree theses.

Dr. Gallion is a Member of the Optical Society of America. He is the Chairman of the IEEE Laser and Electro Optics Society (LEOS) French Chapter. He serves on the Editorial Board and Scientific Committee of several technical publications and as member of program or steering committee of international scientific meetings.